Performance Evaluation of Satellite-Terrestrial Networks

Cognitive Radio and Non-orthogonal Multiple Access

Capstone Report II

Yerassyl Akhmetkaziyev

Nazarbayev University
Department of Electrical and Computer Engineering
School of Engineering and Digital Sciences

This project report was created on the TeXstudio editing platform using LaTeX. All the figures were obtained via MATLAB and drawn using the open-access Origin software tool.

NAZARBAYEV UNIVERSITY

Electrical and Computer Engineering
Nazarbayev University
http://www.nu.edu.kz

Title:
Performance Evaluation of Satellite-Terrestrial Networks

Theme:
Wireless Communications

Project Period:
Spring Semester 2021

Project Group:

Participant(s):
Yerassyl Akhmetkaziyev

Supervisor(s):
Galymzhan Nauryzbayev

Copies: 1

Page Numbers: 16

Date of Completion:
April 27, 2021

Abstract:

The Capstone II project investigates non-orthogonal multiple access (NOMA) assisted cognitive satellite-terrestrial network which is practically limited by channel state information mismatch, interference noises, imperfect successive interference cancellation as well as transceiver hardware impairments. Generalized coverage probability expressions for terrestrial NOMA end-users in are estimated taking into account the impact of constraints caused by interference temperature. Finally, obtained results are corroborated by Monte Carlo simulations and compared with the conventional orthogonal multiple access scheme to demonstrate the advantageous performance of the system network under consideration. Furthermore, the deteriorative impact of practical limitations are studied.

Contents

Preface

Satellite-terrestrial networks can be helpful to solve the issue with mobile communication and internet in the rural areas which is a critical problem nowadays due to distant learning and quarantine regime. Furthermore, it has the potential to deter certain distortions and disruptive phenomena in our country's social sphere by creating new employment and reducing economic migration between rural and urban areas. The successful completion and future implementation of this project have the potential to reduce social and economic inequality by providing ubiquitous and high-quality access to the information flow. Inspired by these opportunities, it was decided to work on this project.

I would like to also take this opportunity to express my heartfelt appreciation and special thanks to professor Galymzhan Nauryzbayev, who, despite his busy schedule, took the time to listen, lead, and keep me on track while enabling me to conduct my research with him. I express my deepest thanks to Dr. Sultangali Arzykulov, a Postdoctoral Fellow at King Abdullah University of Science and Technology (KAUST), for taking part in useful discussions, giving necessary advice and guidance to facilitate the research progress. I also want to express special gratitude to the creator of Sci-Hub, Alexandra Elbakyan, for removing all barriers in the way of science. Finally, I sincerely thank my parents, family, loved ones and friends, who provided the support and arranged an environment for comfort study and work. The successfully completed Capstone project would not be possible without all of them.

Nazarbayev University, April 27, 2021

Yerassyl Akhmetkaziyev
<yerassyl.akhmetkaziyev@nu.edu.kz>

Chapter 1

Introduction

Present terrestrial communication networks can provide high-speed internet connections for billions of subscribers in densely populated regions at comparatively low prices, as the growth of wireline and wireless infrastructure accelerates. However, owing to the infeasibility of terrestrial networks, a substantial number of people in rural areas continue to be unable to access the Internet. In this respect, satellite communications can be seen as an essential component of future networks because they are able to offer uninterrupted access to people all over the world. Satellite networks are able to provide a significant improvement in the forms of fixed and mobile satellite systems due to their pervasive dominance in providing better quality of service (QoS) at a comparatively little cost to customers. Moreover, due to their potential to provide a service to villages and remote locations where the deployments of conventional terrestrial or cellular infrastructures are imprudent or impossible, hybrid satellite-terrestrial networks (STNs) have gained a lot of interest from academia and business. Furthermore, STNs are seen as a potential facilitator of upcoming fifth-generation (5G) communication environment, which are forecasted to see a 1000-fold rise in data traffic [1]. As a result, a serious question of bandwidth scarcity arises [2]. One of the promising solutions can be adopting a cognitive radio (CR) technology in STNs, that allows satellite and terrestrial networks to share bandwidth [3].

Another criterion for the successful implementation of 5G is massive connectivity. Traditionally, satellite-terrestrial systems principally exploit orthogonal multiple access (OMA) method for delivering services; however, due to their orthogonality, it is regarded one of the bottlenecks because the number of servable users is limited. Therefore, the non-orthogonal multiple access (NOMA) technique is recently gaining attention as a promising enabler in the upcoming wireless communication systems by cause of its capability to maintain resource sharing (i.e., time, code, and frequency) at the same time distincting the end-users on the basement of various levels of power [4]. In [5] and [6], the underlay CR and NOMA were

jointly studied aiming at reducing the interference and more effective spectrum utilization. For instance, in [5], the authors evaluated the CR-NOMA in terms of outage by employing an amplify-and-forward relays while a similar network model was studied assuming the detect-and-forward technique over generalized $\alpha - \mu$ fading channels in [6].

However, only a few studies have looked into the efficiency of NOMA in cognitive STNs (CSTNs). For example, for a decode-and-forward relay protocol, the authors in [7] acquired closed-form and asymptotic outage probability (OP) equations of the primary and secondary end-users, whereas a analogous framework was evaluated using ergodic capacity performance metric and utilizing amplify-and-forward protocols in [8]. In addition, authors in [9] derived closed-form OP considering interference temperature constraints (ITC). Consequently, these studies demonstrate that NOMA systems outperform traditional OMA schemes. The authors in [10] investigated the dominance of the NOMA-assisted overlay multi-user CSTN over conventional benchmark schemes involving time division multiple access (TDMA) and direct satellite schemes. In addition, the impact of the PA component was considered, which is used to impose the signals of primary receivers, on the output of the device model in question. They suggest a guideline for estimating the efficient rate of the spectrum exchange configurations based on this research. In the same manner, in [11], in order to attain performance parity among users, coverage fairness-based power allocation (PA) factors of primary and secondary NOMA end-users were given. Furthermore, in [12], the authors used Meijer-G functions to extract analytical expressions for the NOMA-based CSTNs' ergodic capacity, confirming its superiority over conventional TDMA schemes. They also test the system's output by modifying various network specifications such as terrestrial and satellite connection parameters, as well as PA factors.

Thus, this Capstone project investigates the cognitive NOMA-based STN taking into account the successive interference cancellation (SIC), aggregate transceiver distortions, channel and hardware impairment (HI) as well as ITC. Hence, the key contributions of this Capstone project are as follows. First, for the proposed cognitive NOMA-based STN, closed-form coverage probability (CP) expressions are derived for terrestrial network users. Second, using derived analytical results, the impact of multiple system impairments on network performance is analyzed, and the benefit of NOMA is confirmed by contrasting NOMA users' CP performance to a benchmark OMA scheme. The Monte Carlo simulation also validates the accuracy of the obtained analytical findings. The rest of the report is organized as following. First, the system model of our proposed cognitive STN is described with appropriate channel, received signal and SINR models. Then, the derivation steps for the CP considering ITC are provided. Further, in the numerical results section, the degenerative impact of practical limitations are discovered. Finally, we summarize the conducted analysis and provide ideas for future works.

Chapter 2

NOMA-based Cognitive STN

2.1 System model

We examine the downlink underlay multi-user CSTN model, which includes primary and secondary networks as in Fig. 2.1. The primary network (PN) consists of the satellite transmitter (T) which intents to directly communicate with multiple primary users (PUs), indicated by $R_k,\ k \in \{1, 2, \ldots, K\}$. At the same time, the secondary network (SN) consists of a terrestrial base station (S), which can access the licensed band spectrum of PUs and communicate with the secondary users (SUs), denoted by $U_n,\ n \in \{1, 2, \ldots, N\}$. In this situation, the PUs can be affected by S's aggregate interference, while T's interference affects the SUs.

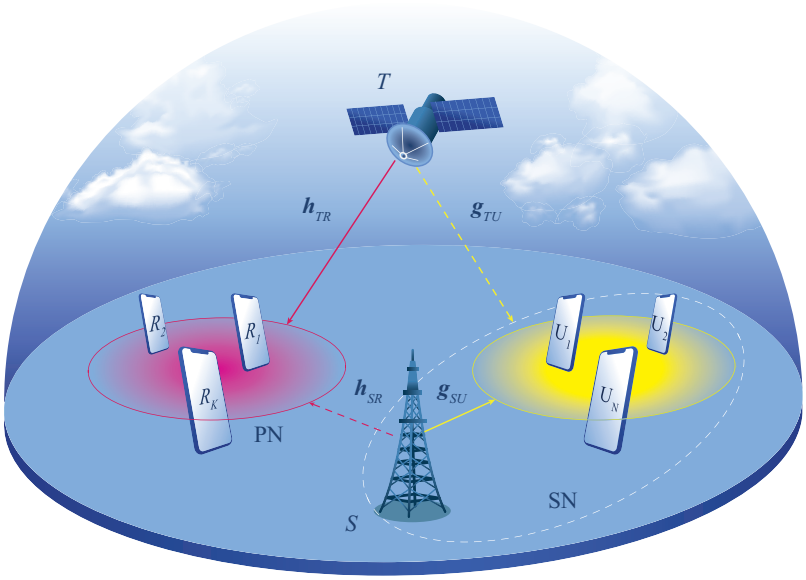

Figure 2.1: Cognitive NOMA-assisted STN model.

2.1.1 Channel Models

We model the communication links using linear minimum mean square error channel estimator as [13],

$$\chi = \tilde{\chi} + \epsilon, \tag{2.1}$$

where χ represents observed mismatched channel, while $\tilde{\chi}$ is the actual channel approximation and ϵ denotes the measurement error, with $\mathcal{CN}(0, \lambda)$, where λ is defined taking into account the formal transmitting SNR ω, as $\lambda = \Phi\omega^{-\eta}$. If $\eta \to \infty$ for $\omega > 0$ then we can obtain an ideal CSI. Furthermore, additive white Gaussian noise (AWGN) exposes all the receiving nodes with mean zero and variance σ^2.

Satellite Interference Channel

The satellite-associated interference link is denoted by $\mathbf{g}_{TU} = [g_{T1}, g_{T2}, \ldots, g_{TN}]$ and $\mathbf{h}_{TR} = [h_{T1}, h_{T2}, \ldots, h_{TK}]$ and they are obeyed by shadowed-Rician fading. Thus, the corresponding probability density function (PDF) is represented by [14]

$$f_{|\chi_k|^2}(x) = \sum_{\ell=0}^{m_k-1} \Upsilon x^{\ell} e^{-\partial_k x},\ x \geq 0, \tag{2.2}$$

with $\Upsilon = \frac{1}{2\bar{b}_k}\left(\frac{2\bar{b}_k m_n}{2\bar{b}_k m_k+\Omega_k}\right)^{m_k} \frac{(1-m_k)_\ell(-\delta_k)^\ell}{(\ell!)^2}$ and $\partial_k = \varrho_k - \delta_k$, where $\delta_k = \frac{\Omega_k}{2\bar{b}_k(2\bar{b}_k m_k+\Omega_k)}$, $\varrho_k = \frac{1}{2\bar{b}_k}$. Here, $2\bar{b}_k$ is the average power of a multi-path component, Ω_k gives the average power of a line-of-sight (LoS) component, and m_k shows the Nakagami parameter. Furthermore, the path-loss for satellite communication connections, L, has linear dependency with logarithmic distance, as stated by Friis' law for free-space propagation [15]. Without sacrificing generality, the distances between satellite and terrestrial clients are believed to be equivalent.

Now, let us identify the satellite antenna gains, G_T. Our antenna array can be characterized by three parameters. First, the angle between the i-th end-user's position and the beam core with respecto to the satellite is represented by φ. Then, we can adopt the beam gain $G_i(\varphi)$ from [16] as $G_i(\varphi) = G_{i,\max}\left(\frac{J_1(u)}{2u} + 36\frac{J_3(u)}{u^3}\right)^2$, where our second parameter, $u = 2.07\frac{\sin\varphi}{\sin\varphi_{3\text{dB}}}$, and the third parameter, $\varphi_{3\text{dB}}$, represents the beam's constant 3-dB angle and $J_l(\cdot)$ denotes the first-kind Bessel function of order l.

Terrestrial Direct Channel

Here, $\mathbf{g}_{SU} = [g_{S1}, g_{S2}, \ldots, g_{SN}]$ and $\mathbf{h}_{SR} = [h_{S1}, h_{S2}, \ldots, h_{SK}]$ represent the terrestrial channels and follow the Nakagami-m fading model. Thus, the channel gains (*i.e.*,

squared values) are Gamma random variables (RVs) with the PDF expressed as

$$f_{|\chi_n|^2}(y) = \frac{y^{m_n-1}e^{-\frac{y}{\nu}}}{\Gamma(m_n)\nu^{m_n}}, \tag{2.3}$$

here m_n represents the Nakagami shape parameter and ν is Nakagami scale parameter.

Furthermore, analog beamforming between communicating nodes was modeled using the sectored antenna pattern as $G(\theta) = G_m$, when $\theta \leq \theta_b$; otherwise, $G(\theta) = G_s$. Particularly, here G_m represents the main lobe gain while G_s inidcates the side lobe gain. In the frame of specified main or side lobe sectors, an antenna gain is assumed to be constant. The angle of a boresight path is θ, and the antenna beamwidth is θ_b. For simplicity, it is presumed that the base station intrudes the users of primary network with side lobe gain, whereas the terrestrial direct links employ main lobe gain.

2.1.2 Signal and SINR Models

The base station S and N NOMA users constitute the terrestrial SN, and the superimposed signal $s = \sum_{n=1}^{N} \sqrt{\beta_n} s_n$ is transmitted to all expected SUs, where s_n and β_n denote the message devoted to the n-th SU and the associated PA coefficient (with $\beta_1 > \beta_2 > \ldots > \beta_N$ s.t. $\sum_{n=1}^{N} \beta_n = 1$), respectively. Hence, considering the CSI (2.1) and hardware impairments, the received signal at U_j, for $j \in \{1, \ldots, N\}$, can be expressed as

$$r_j = \left(\tilde{g}_j + \epsilon\right) \sqrt{P_S G_S G_{D_j} d_j^{-\tau}} \left(\sum_{n=1}^{N} \sqrt{\beta_n} s_n + \bar{\mu}_i \right) + g_{PD} \sqrt{P_T G_T G_D(\varphi) L} \left(x_n + \mu_j\right) + w_j, \tag{2.4}$$

where the influence of residual HIs by the aggregate distortion noises are represented as $\mu_j \sim \mathcal{CN}\left(0, \kappa_j^2\right)$ and $\bar{\mu}_j \sim \mathcal{CN}\left(0, \bar{\kappa}_j^2\right)$, with κ_j and $\bar{\kappa}_j$ denoting compound HI levels present in the communication channels of corresponding transmitter-receiver pairs. Furthermore, $w_j \sim \mathcal{CN}\left(0, \sigma_j^2\right)$ is devoted to the AWGN term. Then, taking into account non-ideal SIC, the corresponding signal-to-interference-noise-distortion ratio (SINDR) at U_j, for $j \in \{1, \ldots, N\}$, to catch message s_n from base station can be expressed as

$$\psi_{j \to n} = \frac{W_1 Z_j P_S}{P_S \left(W_2 Z_j + E\right) + C Q_j + \sigma_j^2}, \tag{2.5}$$

where for the convenience we have introduced certain denotations such as $W_1 = \beta_n G_S G_{D_j} d_j^{-\tau}$ and $W_2 = G_S G_{D_j} d_j^{-\tau} \bar{\mathcal{A}}$ representing the SIC-based interference, with $\bar{\mathcal{A}} = \left(\Psi_n + \tilde{\Psi}_n + \bar{\kappa}_j^2\right)$, where $\Psi_n = \sum_{t=n+1}^{N} \alpha_t$, and $\tilde{\Psi}_n = \sum_{l=1}^{n-1} \xi_l \alpha_l$, with $0 \leq \xi \leq 1$

[6]. Moreover, the channels are denoted as $Z_j = |\tilde{g}_j|^2$, $Q_j = |g_{T_j}|^2$. The power level of channel error (*i.e.*, σ_ϵ^2) is shown by $E = G_S G_{D_j} d_j^{-\tau} \left(1 + \bar{\kappa}_i{}^2\right) \sigma_\epsilon^2$. Furthermore, the interference from the satellite is expressed by $C = \left(1 + \kappa_{T_j}^2\right) P_T G_T G_D(\varphi) L$. Here κ_j and $\bar{\kappa}_j$ denote the compound levels of hardware impairments in the transmission sessions between the respective transceivers. It should be noted that U_1 decodes its own message by considering messages' of the other users as a noise and defining $\Psi_1 = \sum_{t=2}^{N} \alpha_t$ and $\tilde{\Psi}_1 = 0$. Contrarily, U_N has to decode message x_N, provided that $\Psi_N = 0$ and perfect/imperfect SIC realizations expressed by $\tilde{\Psi}_n = \sum_{l=1}^{n-1} \xi_l \alpha_l$.

2.2 Coverage Probability

This section focuses on obtaining an exact closed-form solution for the CP constrained by real-world limitations such as hardware distortion, interference noises, and faulty SIC/CSI conditions. The probability of the SINDR to be greater than a certain threshold value is known as coverage, and this SNR threshold can be expressed as $v = 2^{\mathcal{R}} - 1$, where $\mathcal{R}$ is the data rate threshold [17].

Thus, it is possible to derive the CP for U_N employing (2.5) and taking into account ITC as in (2.6), where $S_i = \frac{I_{\text{ITC}}^{[i]}}{Y_i}$ and $P_S = \min\left(\bar{P}_S, S^*\right)$ by assuming $S^* = \min(S_1, S_2, \ldots, S_N)$. Moreover, we assume $I_{\text{ITC}}^{[i]} = I_{\text{ITC}} d_{SR_i}^{\tau}$ and $Y_i = |h_{SR_i}|^2$, then the CP of terrestrial NOMA-user is given as follows

$$\begin{aligned}
\mathbb{P}_{\text{cov,j}}^{\text{STN}}(v) &= \Pr\left(\frac{W_1 Z_j P_S}{P_S\left(W_2 Z_j + E\right) + C Q_j + \sigma_j^2} > v, \bar{P}_s < S_i\right) \\
&\quad + \Pr\left(\frac{W_1 Z_j S_i}{S_i\left(W_2 Z_j + E\right) + C Q_j + \sigma_j^2} > v, \bar{P}_s > S_i\right) - 1 \\
&= \underbrace{\Pr\left(Z_j > (T_1 + T_2 Q_j), Y_i < \Lambda\right)}_{A} + \underbrace{\Pr\left(Z_j > (J_1 Y_i + J_2 Q_j Y_i + J_3), Y_i > \Lambda\right)}_{B} - 1 .
\end{aligned} \tag{2.6}$$

Further, the expression is simplified with certain denotations for the sake of brevity: $T_1 = \frac{v(E P_s + \sigma_j^2)}{P_s(W_1 - v W_2)}$, $T_2 = \frac{vC}{P_s(W_1 - vW_2)}$, $J_1 = \frac{v\sigma_j^2}{I_{\text{ITC}}^{[i]}(W_1 - vW_2)}$, $J_2 = \frac{vC}{I_{\text{ITC}}^{[i]}(W_1 - vW_2)}$, $J_3 = \frac{v I_{\text{ITC}}^{[i]} E}{I_{\text{ITC}}^{[i]}(W_1 - vW_2)}$, $\Lambda = \frac{I_{\text{ITC}}^{[i]}}{\bar{P}_s}$. To be concise the closed-form coverage probability expression can be presented as a sum of two separate terms, namely, A (2.7) and B (2.8).

$$A = 1 - \left(\sum_{\ell=0}^{m_k-1} \Upsilon \ell! \partial_k^{-\ell-1} - \sum_{\ell=0}^{m_k-1} \sum_{p=0}^{m_0-1} \sum_{n=0}^{p} M_A T_2^n \Upsilon \right.$$
$$\left. \times (n+\ell)! \left(\frac{T_2}{\nu_0} + \partial_k \right)^{-n-\ell-1} \right) \frac{\gamma\left(m, \frac{\Lambda}{\nu}\right)}{\Gamma(m)}. \tag{2.7}$$

$$B = -\frac{\Gamma\left(m, \frac{\Lambda}{\nu}\right)}{\Gamma(m)} \sum_{\ell=0}^{m_k-1} \Upsilon \ell! \partial_k^{-\ell-1} + \sum_{p=0}^{m_0-1} \sum_{t=0}^{p} M_B \sum_{i=0}^{t} \binom{t}{i} J_1^{t-i} J_2^i \frac{\Gamma(t+m)}{\Gamma(m)\nu^m} e^{-\left(\frac{1}{\nu}+\frac{J_1}{\nu_0}\right)\Lambda}$$
$$\times \sum_{\ell=0}^{m_k-1} \sum_{j=0}^{t+m-1} \frac{\Lambda^j \Upsilon}{j!} \frac{V_2 \Omega^{-(i+\ell+1)}}{\Gamma(-j+t+m)} G_{1,2}^{2,1} \left(\frac{\frac{J_2\Lambda}{\nu_0} + \partial_k}{\Omega} \middle| \begin{matrix} 1-(i+\ell+1) \\ 0, -(i+\ell+1)+(-j+t+m) \end{matrix} \right). \tag{2.8}$$

A full derivation can be found in Appendix A. The numerical results obtained from MATLAB Monte-Carlo simulations are discussed in the following chapter. Different aspects of the network and impact of impairments are examined and studied.

Chapter 3

Results and Discussions

This chapter presents numerical coverage performance results of the network scheme considered in our Capstone, as specified by the simulation framework shown in Table 3.1. Monte Carlo simulations are also used to verify our derived mathematical findings. It should be noted that only two user scenarios are considered for the sake of convenience. Multiple NOMA users might not be possible in real-time communication because of the growing complexity in the processing of the receivers' SIC in a non-linear way as the amount of end-users increases [18]. Furthermore, as the SIC error spreads, this uncertainty becomes much more important [6].

Table 3.1: Simulation parameters.

Parameter	**Value**
Terrestrial antenna gains, $\{G_m, G_s\}$	$\{12, -1.1092\}$ dB
Terrestrial channel parameter, m_0	4
Satellite antenna gains, $\{G_T, G_{i,max}\}$	$\{4.8, 54\}$ dB
Satellite channel parameters, $\{m_i, b_i, \Omega_i\}$	$\{5, 0.251, 0.279\}$
Path-loss exponent, τ	2
Threshold, $\{\zeta_{NOMA}, \zeta_{OMA}\}$	$\{3, 12\}$ dB
PA factors, $\{\alpha_1, \alpha_2\}$	$\{0.7, 0.3\}$
Orbit height, D	35786 km
Interference noise power	10 dB
ST-to-R_K distance, $\{d_{R_1}, d_{R_2}\}$	$\{150, 75\}$ m
ST-to-U_N distance, $\{d_{U_1}, d_{U_2}\}$	$\{100, 50\}$ m
3dB angle, φ_{3dB}	0.4°
Temperature, $\mathcal{T}$	300 K
Carrier frequency, f_c	2 GHz
Carrier bandwidth, $\mathcal{W}$	15 MHz

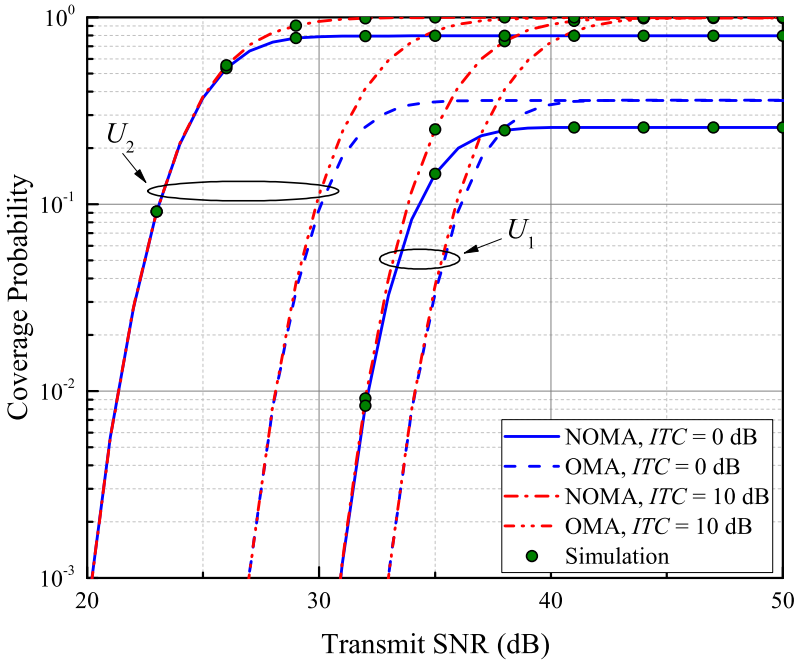

Figure 3.1: The CP versus the transmit SNR for the NOMA and OMA schemes with different $ITC = \{0, 10\}$ dB.

Fig. 3.1 compares the CP of the analytical NOMA network with simulated OMA scheme for both users with two different levels of ITC is demonstrated. The figure demonstrates that the greater value of the ITC results in a stronger CP for NOMA-based networks. When a lower ITC is applied, on the other hand, the CP degenerates by displaying saturation at smaller values of SNR. Furthermore, in terms of CP, the NOMA-based system surpasses the OMA. Nevertheless, in comparison to the rate of SNR for the OMA scheme, the saturation period of CP for the NOMA-assisted system begins at smaller ranks of transmitting SNR for U_1. The ITC equation explains this, with a transmit power of $0.5P_s$ increasing an amount of ITC effect at the base station.

Fig. 3.2 demonstrates the influence of the CSI mismatch for two users in the SN. It also takes into account SNR-independent and SNR-dependent CSI situations. Particularly, the channel error variance is said to be free from the transmit SNR if $\eta = 0$, and in that case Φ is found to have a substantial impact on device efficiency. Interestingly, at low SNR values, Φ has no impact on CP efficiency. Particularly, it starts influencing U_1 distinctively at 35 dB and U_2 at 25 dB, approximately. It happens due to the fact that when Φ approaches 0, the CSI quality tends to become perfect. Therefore, the small mismatch in CSI does not affect the performance at low SNR. Contrarily, CSI is said to be SNR-dependent and achieves saturation only at a greater rate of SNR in comparison with the SNR-independent CSI if we

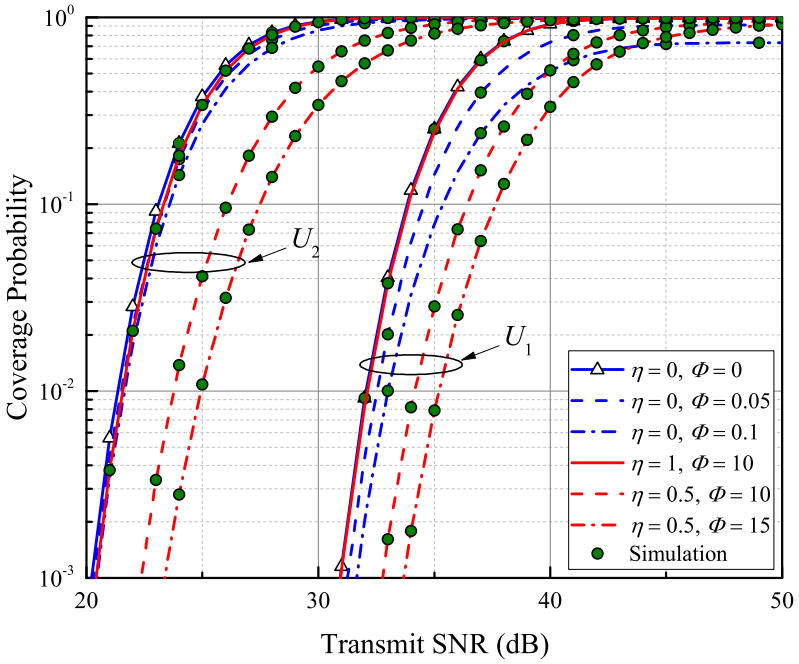

Figure 3.2: The CP versus the transmit SNR for the SN for different CSI scenarios.

set $\eta \neq 0$. The rise in η leads to a boost in system performance, as can be seen. In the situation with equivalent η values, however, increasing Φ provokes a minor deterioration in CP efficiency. Furthermore, it is clear that η has a far greater impact on results than Φ. It's worth noting that at high SNR values, both curves average out at the same CP point.

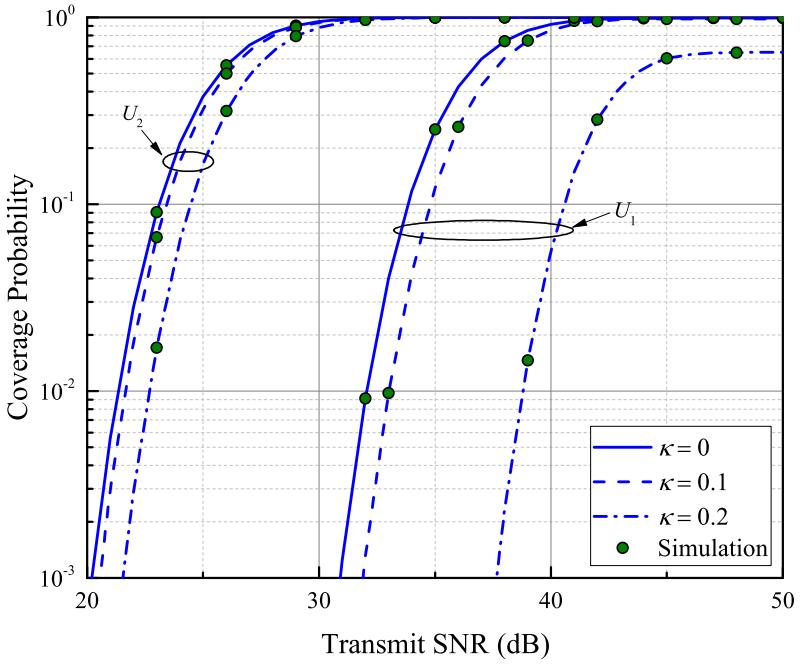

Figure 3.3: The CP versus the transmit SNR for the SN with different HI levels.

Many recent studies have been carried out under the assumption of ideal hardware structures at the transmitting and receiving user nodes. In reality, the hardware suffers from a variety of flaws, including high power amplifiers, phase noises as well as non-linear in-phase and quadrature-phase imbalance. In Fig. 3.3, the impact of various amounts of HIs on the CP efficiency of the terrestrial SN is investigated. The HI amount was specifically configured to three separate scenarios with $\kappa = \{0, 0.1, 0.2\}$. In the presence of HI, both U_1 and U_2's CP degrades noticeably, as predicted. It is worth noting that HIs have a minor effect at low SNRs. Surprisingly, even a low HI value has a marginal effect, particularly for user 2. However, it is clear that a greater value of HI, *i.e.*, $\kappa = 0.2$, significantly degrades overall system performance in terms of CP.

Chapter 4

Conclusion

Satellite networks are regarded as a future infrastructure for smart grid, Internet-of-Things, wireless sensor networks, and space-based cloud as a promising part of the 5G environment. In such situations, future satellite networks are likely to be built into current conventional technologies, and can be broadly distributed using various systems on GEO/LEO satellites to ensure a worldwide coverage, enable advanced 5G scenarios, and minimize operating costs. Thus, in the Capstone project, the performance of cognitive NOMA-based STNs was evaluated where terrestrial SUs enjoy access to spectrum with the satellite PN limited only by interference temperature constraint. We examined NOMA for terrestrial secondary networks, in contrast to previous work, and extracted closed-form CP expressions that considered the SIC/CSI and hardware impairments, as well as noises coming from interference nodes. In addition, a contrast with the conventional OMA network, which is used as a common scheme, confirmed that the planned NOMA-assisted STN achieves excellent efficiency when adequately using the spectrum resource. Moreover, we investigated the deteriorative impact of CSI mismatch of both SNR dependent/independent scenarios as well as hardware imperfections. Finally, Monte Carlo simulations confirmed that the derived analytical results were accurate.

To sum up, it can be said that the work plan for the Capstone project was accomplished successfully. The main milestones of the project achieved by the proposed time and met all the requirements.

In future works, this project can be extended by adding new details (i.e. relay, multiple interference nodes) to the system model. In addition to coverage probability, the efficiency of such a device model can be measured using a variety of metrics, namely, ergodic capacity, throughput, bit error rate, etc.

Bibliography

[1] L. Dai et al. "A Survey of Non-Orthogonal Multiple Access for 5G". In: *IEEE Communications Surveys Tutorials* 20.3 (2018), pp. 2294–2323.

[2] G. Giambene, S. Kota, and P. Pillai. "Satellite-5G Integration: A Network Perspective". In: *IEEE Network* 32.5 (2018), pp. 25–31.

[3] Y. Ruan et al. "Spectral-Energy Efficiency Tradeoff in Cognitive Satellite-Vehicular Networks Towards Beyond 5G". In: *2019 IEEE Wireless Communications and Networking Conference (WCNC)*. 2019, pp. 1–6.

[4] M. Liu, T. Song, and G. Gui. "Deep Cognitive Perspective: Resource Allocation for NOMA-Based Heterogeneous IoT With Imperfect SIC". In: *IEEE Internet of Things Journal* 6.2 (2019), pp. 2885–2894.

[5] S. Arzykulov et al. "Performance Analysis of Underlay Cognitive Radio Nonorthogonal Multiple Access Networks". In: *IEEE Transactions on Vehicular Technology* 68.9 (2019), pp. 9318–9322.

[6] S. Arzykulov et al. "Hardware- and Interference-Limited Cognitive IoT Relaying NOMA Networks With Imperfect SIC Over Generalized Non-Homogeneous Fading Channels". In: *IEEE Access* 8 (2020), pp. 72942–72956.

[7] X. Zhang et al. "Performance Analysis of NOMA-Based Cooperative Spectrum Sharing in Hybrid Satellite-Terrestrial Networks". In: *IEEE Access* 7 (2019), pp. 172321–172329.

[8] X. Zhang et al. "Outage Performance of NOMA-Based Cognitive Hybrid Satellite-Terrestrial Overlay Networks by Amplify-and-Forward Protocols". In: *IEEE Access* 7 (2019), pp. 85372–85381.

[9] Y. Akhmetkaziyev et al. "Cognitive Non-ideal NOMA Satellite-Terrestrial Networks with Channel and Hardware Imperfections". In: *2021 IEEE Wireless Communications and Networking Conference (WCNC)*. 2021, pp. 1–6.

[10] V. Singh, P. K. Upadhyay, and M. Lin. "On the Performance of NOMA-Assisted Overlay Multiuser Cognitive Satellite-Terrestrial Networks". In: *IEEE Wireless Communications Letters* 9.5 (2020), pp. 638–642.

[11] Y. Akhmetkaziyev et al. "Performance of NOMA-Enabled Cognitive Satellite-Terrestrial Networks With Non-Ideal System Limitations". In: *IEEE Access* 9 (2021), pp. 35932–35946.

[12] X. Yan et al. "On the ergodic capacity of NOMA-based cognitive hybrid satellite terrestrial networks". In: *2017 IEEE/CIC International Conference on Communications in China (ICCC)*. 2017, pp. 1–5.

[13] Y. Gao et al. "Analysis of the Dynamic Ordered Decoding for Uplink NOMA Systems With Imperfect CSI". In: *IEEE Transactions on Vehicular Technology* 67.7 (2018), pp. 6647–6651.

[14] A. Abdi et al. "A new simple model for land mobile satellite channels: first- and second-order statistics". In: *IEEE Transactions on Wireless Communications* 2.3 (2003), pp. 519–528.

[15] K. Guo et al. "Outage Analysis of Cognitive Hybrid Satellite-Terrestrial Networks With Hardware Impairments and Multi-Primary Users". In: *IEEE Wireless Communications Letters* 7.5 (2018), pp. 816–819.

[16] P. K. Sharma, D. Deepthi, and D. I. Kim. "Outage Probability of 3-D Mobile UAV Relaying for Hybrid Satellite-Terrestrial Networks". In: *IEEE Communications Letters* 24.2 (2020), pp. 418–422.

[17] G. Nauryzbayev, M. Abdallah, and K. M. Rabie. "Outage Probability of the EH-Based Full-Duplex AF and DF Relaying Systems in $\alpha - \mu$ Environment". In: *2018 IEEE 88th Vehicular Technology Conference (VTC-Fall)*. 2018, pp. 1–6.

[18] Z. Ding, M. Peng, and H. V. Poor. "Cooperative Non-Orthogonal Multiple Access in 5G Systems". In: *IEEE Communications Letters* 19.8 (2015), pp. 1462–1465.

[19] O. L. Alcaraz López et al. "Aggregation and Resource Scheduling in Machine-Type Communication Networks: A Stochastic Geometry Approach". In: *IEEE Transactions on Wireless Communications* 17.7 (2018).

[20] I. S. Gradshteyn and I. M. Ryzhik. *Table of integrals, series, and products*. Seventh. Translated from the Russian, Translation edited and with a preface by Alan Jeffrey and Daniel Zwillinger, With one CD-ROM (Windows, Macintosh and UNIX). Elsevier/Academic Press, Amsterdam, 2007, pp. xlviii+1171. ISBN: 978-0-12-373637-6; 0-12-373637-4.

[21] Wolfram. *The Wolfram functions site*. Last visited on 11/04/2020. URL: \url{http://functions.wolfram.com}.

Appendix A

Closed-form Coverage Probability

The derivation steps of general closed-form expression for evaluating the coverage efficiency of the terrestrial NOMA users are presented in this section. First, let us start with expressing the term A in (2.6) as following

$$A = 1 - \underbrace{\int_{q=0}^{\infty} f_Q(q) \underbrace{\int_{z=0}^{T_1+T_2Q_j} f_Z(z)\mathrm{d}z}_{A_1} \mathrm{d}q}_{A_2} \underbrace{\int_{y=0}^{\Lambda} f_Y(y)\mathrm{d}y}_{A_3}.$$

Here, the letters Z and Y represent the terrestrial associated channels, hence their corresponding PDFs are evaluated using Nakagami-m statistical model. At the same time, Q term indicates the satellite associated channel and its corresponding PDF is modeled using shadowed-Rician distribution. Thus, by employing the PDF in (2.3), we can obtain A_1 as

$$A_1 = 1 - \sum_{p=0}^{m_0-1} \sum_{n=0}^{p} e^{\frac{-T_2Q_j}{\nu_0}} M_A (T_2Q_j)^n, \tag{A.1}$$

here $M_A = e^{\frac{-T_1}{\nu_0}} \frac{1}{\nu_0^p \Gamma(p+1)} \binom{p}{n} T_1^{p-n}$. Consequently, utilizing the PDF in (2.2), A_2 can be evaluated thanks to [20, Eq. (3.351.3)] as

$$\begin{aligned} A_2 &= \left(1 - \sum_{p=0}^{m_0-1} \sum_{n=0}^{p} e^{\frac{-T_2Q_j}{\nu_0}} M_A (T_2Q_j)^n\right) \sum_{\ell=0}^{m_k-1} \Upsilon \int_0^{\infty} q^{\ell} e^{-\partial_k q} \mathrm{d}q \\ &= \sum_{\ell=0}^{m_k-1} \Upsilon \ell! \partial_k^{-\ell-1} - \sum_{\ell=0}^{m_k-1} \sum_{p=0}^{m_0-1} \sum_{n=0}^{p} \left(\frac{T_2}{\nu_0} + \partial_n\right)^{-n-\ell-1} M_A T_2^n \Upsilon (n+\ell)!. \end{aligned} \tag{A.2}$$

Further, the independent term A_3 is calculated as $\frac{\gamma\left(m, \frac{\Lambda}{\nu}\right)}{\Gamma(m)}$. At the end, the final closed-form CP expression of term A can be expressed as (2.7) by inserting A_2 and A_3 into (A).

Now, let us determine the term B in (2.6) as

$$B = 1 - \int_{q=0}^{\infty} f_Q(q) \underbrace{\int_{y=\Lambda}^{\infty} f_Y(y) \int_{0}^{J_1 Y + J_2 Y Q_j + J_3} f_Z(z) \mathrm{d}z \mathrm{d}y}_{B_1} \mathrm{d}q. \tag{A.3}$$

At first, we can calculate B_1 term in Eq. (A.3) by deploying (2.3) and the CDF of Z as following

$$\begin{aligned} B_1 &= \left(1 - e^{\frac{-J_1 Y - J_2 Y Q_j - J_3}{\nu_0}} \sum_{p=0}^{m_0-1} \frac{\left(J_3 + Y(J_1 + J_2 Q_j)\right)^p}{\nu_0^p \Gamma(p+1)}\right) \int_{\Lambda}^{\infty} \frac{y^{m-1} e^{-\frac{y}{\nu}}}{\Gamma(m)\nu^m} \mathrm{d}y \\ &= \frac{\Gamma(m, \frac{\Lambda}{\nu})}{\Gamma(m)} - \sum_{p=0}^{m_0-1} \sum_{t=0}^{p} M_B \left(J_1 + J_2 Q_j\right)^t \int_{\Lambda}^{\infty} \frac{y^t y^{m-1} e^{-y\left(\frac{1}{\nu} + V_1\right)}}{\Gamma(m)\nu^m} \mathrm{d}y \\ &= \frac{\Gamma(m, \frac{\Lambda}{\nu})}{\Gamma(m)} - \sum_{p=0}^{m_0-1} \sum_{t=0}^{p} M_B \underbrace{\left(J_1 + J_2 Q_j\right)^t \frac{\Gamma(t+m, \left(\frac{1+\nu V_1}{\nu}\right)\Lambda)}{\Gamma(m)\nu^m} \left(\frac{1+\nu V_1}{\nu}\right)^{-t-m}}_{B_2}, \end{aligned} \tag{A.4}$$

where $M_B = e^{\frac{-J_3}{\nu_0}} \frac{1}{\nu_0^p \Gamma(p+1)} \binom{p}{t} (J_3)^{p-t}$ and $V_1 = \frac{J_1 + J_2 Q_j}{\nu_0}$. In addition, we must use the upper incomplete Gamma function's series representation, which is given by [20] as $\Gamma(b, c) = \Gamma(b) e^{-c} \sum_{i=0}^{b-1} \frac{c^i}{i!}$ and to extend B_2 in (A.4), binomial theorem has to be used. Thus, by applying the aforementioned methods and after some algebraic manipulations, we can rewrite B_2 as

$$B_2 = \sum_{i=0}^{t} \binom{t}{i} J_1^{t-i} \left(J_2 Q_j\right)^i \sum_{j=0}^{t+m-1} \frac{\Gamma(t+m)\Lambda^j V_2}{\Gamma(m)\nu^m j!} e^{-\left(\frac{1}{\nu} + \frac{J_1 + J_2 Q_j}{\nu_0}\right)\Lambda} \left(1 + \Omega Q_j\right)^{j-t-m}, \tag{A.5}$$

where $\Omega = \frac{\nu J_2}{\nu_0 + \nu J_1}$ and $V_2 = \left(\frac{\nu_0 + \nu J_1}{\nu_0 \nu}\right)^{j-t-m}$. Then, we can rewrite the term B as

$$\begin{aligned} B = 1 &- \frac{\Gamma(m, \frac{\Lambda}{\nu})}{\Gamma(m)} \sum_{\ell=0}^{m_k-1} \mathrm{Y} \int_{0}^{\infty} q^{\ell} e^{-\partial_k q} \mathrm{d}q - \sum_{p=0}^{m_0-1} \sum_{t=0}^{p} M_B \\ &\times \sum_{i=0}^{t} \binom{t}{i} J_1^{t-i} J_2^i \frac{\Gamma(t+m)}{\Gamma(m)\nu^m} e^{-\left(\frac{1}{\nu} + \frac{J_1}{\nu_0}\right)\Lambda} \sum_{\ell=0}^{m_k-1} \sum_{j=0}^{t+m-1} \frac{\Lambda^j}{j!} V_2 \mathrm{Y} \\ &\times \int_{0}^{\infty} \left(1 + \Omega Q_j\right)^{-(t+m-j)} q^{i+\ell+1-1} e^{-\left(\frac{J_2 \Lambda}{\nu_0} + \partial_k\right) q} \mathrm{d}q. \end{aligned} \tag{A.6}$$

At the end, by applying the Meijer-G function, which is defined in [21, Eqs. (7.34.3.46.1) and (7.34.3.271.1)], where $(1 + c\gamma)^{-d} = \frac{1}{\Gamma(d)} G_{1,1}^{1,1}\left(c\gamma \big|_0^{1-d}\right)$ and $e^{-b\gamma} = G_{0,1}^{1,0}\left(b\gamma \big|_0^{-}\right)$, the closed-form CP expression of term B is derived after some basic mathematical manipulations with the additional help of [20, Eq. (3.351.3)] as in (2.8).